

Evolutionary synthesis modeling of red supergiant features in the near-infrared

Livia Origlia

Osservatorio Astronomico di Bologna, Via Zamboni 33, I-40126 Bologna, Italy
e-mail: origlia@astbo3.bo.astro.it

and

Space Telescope Science Institute, 3700 San Martin Drive, Baltimore, MD 21218

Jeffrey D. Goldader, Claus Leitherer, and Daniel Schaerer

Space Telescope Science Institute, 3700 San Martin Drive, Baltimore, MD 21218
e-mail: goldader@stsci.edu, leitherer@stsci.edu, schaeerer@stsci.edu

and

Ernesto Oliva

Osservatorio Astrofisico di Arcetri, Largo E. Fermi 5, I-50125 Firenze, Italy
e-mail: oliva@arcetri.astro.it

ABSTRACT

We present evolutionary synthesis models applied to near-infrared spectral features observed in the spectra of young Magellanic Cloud clusters and starburst galaxies. The temporal evolution of the first and second overtones of CO at $2.29 \mu\text{m}$ (2–0 bandhead) and $1.62 \mu\text{m}$ (6–3 bandhead) and of the $(U - B)$, $(B - V)$ and $(J - K)$ colors are investigated.

We find that the current evolutionary tracks of massive stars with sub-solar chemical composition in the red supergiant phase are not reliable for any synthesis of the temporal evolution of infrared stellar features.

The high sensitivity of the selected infrared features to the atmospheric parameters of cool stars allows us to place constraints on the temperature and the fraction of time spent in the red part of the Hertzsprung–Russell diagram by massive stars during their core–helium burning phase.

We derive a set of empirically calibrated spectrophotometric models by adjusting the red supergiant parameters such that the properties of the observed templates are reproduced.

Subject headings: stars: supergiants — galaxies: evolution — galaxies: starburst — galaxies: stellar content — infrared: galaxies

Accepted for publication in ApJ

1. Introduction

Since Tinsley's (1972) pioneering work, various evolutionary synthesis models of stellar populations in galaxies have been developed, using improved theoretical and empirical spectral libraries for better comparisons between predicted and observed spectrophotometric properties of galaxies. A comprehensive compilation of the available models was published by Leitherer et al. (1996).

Galaxies with dominant young stellar populations ($\lesssim 100$ Myr) are called 'starbursts' (Searle, Sargent, & Bagnuolo 1973). An overview of the properties of the stellar content of starburst galaxies can be found in Leitherer (1996). Moorwood (1996) reviewed starburst galaxies with particular emphasis on infrared (IR) aspects.

Substantial theoretical and observational efforts have been made to calibrate suitable ultraviolet (UV) and optical diagnostics for studying the stellar content of starburst galaxies (Leitherer et al. 1996). Massive stars have only few and comparatively weak features in the optical spectral region. Furthermore, most absorption lines are blended with nebular emission lines if the stars are embedded in ionized gas. Notable exceptions are the strong hot-star wind features in the UV (Leitherer, Robert, & Heckman 1995) and the Wolf-Rayet feature at 4650/4686 Å, which has been used to define a subset of starbursts called Wolf-Rayet galaxies (Conti 1991). Wolf-Rayet stars are massive stars at the end point of their evolution (Abbott & Conti 1987). Attempts to utilize Wolf-Rayet features for constraining the stellar population have been made (e.g., Meynet 1995; Schaerer 1996; Schaerer & Vacca 1998) although uncertainties in their modeling re-

main.

Only recently has such a systematic analysis been extended to the near-IR range where red supergiants (RSGs) dominate. This spectral range is of particular interest to the modeling of starburst spectra. RSGs are less evolved than Wolf-Rayet stars, and therefore their evolutionary status is thought to be better understood. The main features in the IR spectra of integrated stellar systems are absorption lines due to neutral metals and molecules (e.g., Kleinmann & Hall 1986; Origlia et al. 1993, hereafter OMO93) tracing red stellar populations, and the hydrogen recombination lines of the Paschen and Brackett series, which mainly provide information on the number of ionizing photons. Once the first RSGs have formed, the near-IR spectra of starbursts show their characteristic absorption features. Due to the fast technological improvements in IR array performances, near-IR spectra of stellar clusters and galaxies showing RSG features are becoming available in increasing numbers (e.g., Lançon & Rocca-Volmerange 1992; Goldader et al. 1995, 1997; Oliva et al. 1995; Smith et al. 1996; Oliva & Origlia 1998, hereafter OO98).

When dealing with integrated populations, one of the most critical issues in properly classifying their stellar content is the disentanglement of age and metallicity effects (cf. e.g., the review by Renzini 1986 and, more recently, Worthey 1994). OMO93 discussed the behavior of the near-IR CO features at $\lambda 1.62$ and $\lambda 2.29$ in individual red stars with varying stellar parameters such as effective temperature, gravity, metallicity, and microturbulent velocity. The results of OMO93, combined with theoretical models for the dependence of these parameters on stellar age and mass, of-

fer the opportunity to make predictions for the strength of RSG spectral features during the times when massive RSGs dominate in starbursts, i.e. from about 8 to 30 Myr.

In this paper, we couple the new near-IR spectral diagnostics of OMO93 to evolutionary synthesis models based on those of Leitherer & Heckman (1995, hereafter LH95 and Leitherer et al. 1998, hereafter L98). The technique is outlined in § 2. Results of the numerical simulations and the confrontation with observations are in § 3. Empirical modifications to the RSG models which lead to near-IR features in better agreement with observations are discussed in § 4. Our conclusions are presented in § 5.

2. Synthesis technique

All models in this paper were constructed using an updated evolutionary synthesis code based on that of LH95. The new code is described in detail by L98. Briefly, the code now incorporates the most recent stellar evolutionary tracks from the Geneva group at $Z=0.04$, 0.020, 0.008, 0.004, and 0.001 (Schaller et al. 1992; Schaerer et al. 1993). It has also been updated to allow the use of isochrone synthesis. Finally, the corrected grid of atmospheres compiled by Lejeune, Cuisinier & Buser (1997) is used. This atmosphere grid reproduces the observed effective temperature *versus* color relation at all metallicities.

As with the LH95 code, the new version allows the star formation rate to be one of two cases. First, stars could form in an *instantaneous burst* from interstellar gas of mass M_{tot} with no subsequent star formation. Alternatively, the models allow for *continuous star formation*, at a constant level determined by the star formation rate in $M_{\odot} \text{ yr}^{-1}$. The stellar population is distributed along the zero-

age main sequence following an initial mass function (IMF) which we parameterize as

$$\phi(M) = \frac{dN}{dM} = CM^{-\alpha} \quad (1)$$

between the upper and lower cutoff masses, M_{up} and M_{low} , respectively. The normalization constant C is determined by the total stellar mass. $\alpha = 2.35$ corresponds to the classical Salpeter (1955) value.

Each star is tracked in the Hertzsprung-Russell diagram (HRD) from the zero-age main sequence until its death. Effective temperatures T_{eff} , surface gravities $\log g$, and surface abundances are assigned during each time step and appropriate model atmospheres are chosen.

[Z/Fe]=0 at all metallicities¹ are adopted in both the model atmospheres and in the evolutionary models. The nebular continuum (bound-free, free-free, and two-photon) is computed and added to the stellar continuum. Thus, dilution of stellar spectral features by the nebular continuum is accounted for.

For the present study we enhanced the code by implementing the theoretical equivalent widths of CO $\lambda 1.62$ and $\lambda 2.29$ from OMO93. Their models predict these indices as a function of T_{eff} , $\log g$, microturbulent velocity ξ , and metallicities between 1/100 and 3 times solar. These indices are successful in reproducing the corresponding observed spectra of both single giant and supergiant stars (OMO93), and integrated stellar clusters with known parameters in both our Galaxy (Origlia et al. 1997) and the Magellanic Clouds (OO98). The equivalent

¹Throughout this paper we define metallicity as the mass fraction of all elements heavier than helium. The sun has $Z=0.020$ in this definition.

widths were obtained at each time step from a multi-dimensional interpolation in the spectral grids.

At temperatures less than 3000 K we set the indices to the value at the lowest tabulated temperature, with all other parameters held constant; at temperatures higher than 4500 K, we set the indices to zero. These assumptions are reasonable since at temperatures higher than 4500 K the CO molecule is almost dissociated, hence the equivalent widths of the selected features become very small. Similarly, the CO temperature dependence becomes negligible below 3600 K (OMO93), and the equivalent widths of the selected lines do not change significantly at lower temperatures.

A large grid of models was run exploring the following parameter space:

- Instantaneous burst and continuous star formation models.
- Ages < 25 Myr.
- Metallicities $Z = 0.020$ ($=Z_{\odot}$), $Z = 0.008$ ($=40\%$ solar).
- IMF with slopes $\alpha = 2.35$ and 3.3 .
- $M_{\text{up}} = 100 M_{\odot}$; $M_{\text{low}} = 1 M_{\odot}$.
- Microturbulent velocities of 3 and 5 km s $^{-1}$, typical for RSGs (e.g., Tsuji et al. 1994; OO98, and references therein).
- Solar and non-solar $[C/Fe]$, where C was depleted by 0.5 dex. Carbon is expected to be slightly depleted (e.g., Lambert et al. 1984) due to internal mixing in post-main-sequence stages.

The changes in microturbulent velocity and $[C/Fe]$ abundances were kept internal to the

routine in which the values of the indices were computed, and have no effect on other values calculated by the code (e.g., colors).

The near-IR properties of stellar populations dominated by RSGs are rather insensitive to variations of M_{up} between 30 and 100 M_{\odot} (cf. LH95). This results from the small number of RSGs evolving from stars with progenitor masses above $\sim 30 M_{\odot}$.

3. Results from standard RSG models

In this section we highlight the key results of our simulations. We show models for the CO $\lambda 1.62$ and $\lambda 2.29$ features and $(U - B)$, $(B - V)$ and $(J - K)$ colors and we compare the results to two sets of observational data: a sample of Large Magellanic Cloud (LMC) clusters and starburst galaxies.

3.1. Observational templates

We selected the 5 young LMC clusters NGC1818, NGC1984, NGC1994, NGC2004 and NGC2011 with measured CO features from OO98. 3 clusters from the OO98 sample were excluded. NGC1866 and NGC1987 are too old to harbor massive RSGs, and NGC330 is in the SMC with a much lower metallicity. Optical colors are from van den Bergh (1981), extinction and the $(J - K)$ color are from Persson et al. (1983). The uncertainties of the CO features and color are 0.3–0.5 Å and ≤ 0.1 mag, respectively, as discussed in the cited literature. The same measurement errors apply to the starburst sample further below. A range of ages has been assigned to each cluster according to the estimates from different authors (Hodge 1983; Elson & Fall 1985, 1988; Girardi et al. 1995; Cassatella et al. 1996).

The metallicity of individual young LMC

clusters is not accurately known (cf. e.g. the compilation by Sagar & Pandey 1989) but on average values well below solar are inferred. For the selected clusters several independent estimates based on optical and infrared spectra (cf. Richtler, Spite & Spite 1989; Reitermann et al. 1990; Jasiewicz & Thévenin 1994; OO98) indicate values between one tenth and at most half solar.

The selected sample of starburst galaxies with measured spectral features is the one observed by Oliva et al. (1995). The galaxies are NGC253, NGC1614, NGC1808, NGC3256, NGC4945, NGC7552, and NGC7714. We also added NGC1705 to this sample, a well studied galaxy with colors from Lamb et al. (1985) and Quillen, Ramirez & Frogel (1995). For these galaxies we also used $(U - B)$ and $(B - V)$ colors from Veron-Cètty (1984) and Hamuy & Maza (1987) and the $(J - K)$ color from Glass & Moorwood (1985). The colors were corrected for extinction assuming an intrinsic $(J - H)$ in the range 0.6–0.7 (cf. e.g., Scoville et al. 1985) and the interstellar extinction law by Rieke & Lebofsky (1985) for a homogeneous dust distribution. The de-reddened values are quite uncertain due to the amount of the correction and its aperture-size dependence, particularly in the case of the $(U - B)$ and $(B - V)$. Our main arguments will therefore be based on the equivalent widths of the near-IR features, which are reddening independent. The presence of RSGs in the central region of these galaxies (Oliva et al. 1995) indicates a burst age (as traced by RSGs themselves and by the Brackett lines) in the range between 10 and 100 Myr. The inferred light to mass ratios seem also to suggest that there is no significant contamination by an underlying, older stellar population, which would dilute

the observed features. Hot dust, if present, could dilute the spectral features as well. OMO93 used the ratio of $\text{CO}\lambda 1.62/\text{Si}\lambda 1.59$ and $\text{CO}\lambda 1.62/\text{CO}\lambda 2.29$ to quantify the degree of dust dilution. Oliva et al. (1995) applied this method to the starburst sample discussed in this paper and found no significant dust dilution in the central few arcseconds.

The metal abundance of starbursts is poorly known and the available estimates vary by up to an order of magnitude, depending on the element used to trace metallicity, the galaxy sampled region, the observational technique and the spectral synthesis modeling. As an example, for NGC253 values ranging between less than one tenth up to about solar have been proposed (cf. e.g. Webster & Smith 1983; Carral et al. 1994; Zaritsky, Kennicutt & Huchra 1994; Arimoto et al 1997; Ptak et al. 1997; OO98). Nevertheless, in our sample there at least two objects whose metallicity is better constrained in the range 0.3–0.5 solar, namely NGC1705 (Storchi-Bergmann, Calzetti & Kinney 1994) and NGC7714 (González-Delgado et al. 1995; García-Vargas et al. 1997; OO98).

The star-formation histories in the LMC clusters are most likely close to the idealized case of an instantaneous burst, as suggested by their small sizes of a few pc. This makes them the simplest stellar systems for comparisons with models. Starburst galaxies are more complex, with typical size scales of \sim kpc. By averaging over such large regions, most of the time information is lost, and the star formation history can be approximated by a steady-state model. The relatively small color and equivalent width range observed for starbursts suggest a steady-state situation as well. As opposed to the LMC cluster sample, the starbursts were not selected by their ages.

Therefore it would be difficult to understand why they fall into a very narrow parameter range, which, for a given metallicity, would indicate equal ages in instantaneous models. For simplicity and as two possible extreme situations in the plots we compared pure instantaneous bursts with stellar clusters and continuous star-formation models with galaxies.

3.2. Spectroscopic indices and colors

The temporal variation of the equivalent widths of the selected CO $\lambda 1.62$ and $\lambda 2.29$ features predicted by our models for both an instantaneous burst and continuous star formation using a Salpeter IMF are plotted in Figs. 1 and 2 for solar and 40% solar metallicities, respectively. The corresponding values measured in the selected LMC clusters and starburst galaxies are plotted for comparison, as well.

The $(U - B)$, $(B - V)$ and $(J - K)$ colors of the $Z = 0.020$ and $Z = 0.008$ models and the corresponding, de-reddened values measured in the LMC clusters and starburst galaxies are plotted in Fig. 3. The relative large spread in color shown by the LMC clusters (a few tenths of magnitude) can be ascribed mainly to age and/or metallicity effects and some uncertainty in the reddening correction. In the case of starbursts the main uncertainty is the adopted reddening correction, as already mentioned above.

From the comparison of models and observational templates we find that the observed CO features and $(J - K)$ colors can only be reproduced by models with metallicity very close to solar. Theoretical curves at 40% solar metallicities systematically predict too weak CO features and blue $(J - K)$ colors for all objects but NGC1818 and NGC1984 which, however, are known to have metallicities

$\leq 20\%$ solar.

The discrepancy between models and observations becomes even more severe when the latter are compared with continuous star formation models, which significantly underestimate (by up to a factor of two) the equivalent widths of the observed CO features and the $(J - K)$ color.

Both the 40% and solar metallicity models can reasonably fit the observed $(B - V)$ colors, while the behavior of the $(U - B)$ color is more complex, being redder than observed in the case of an instantaneous burst and bluer than observed in the case of continuous star formation.

3.3. Why does the standard RSG model fail?

By comparing theoretical predictions and observations of both LMC clusters and starburst galaxies with sub-solar metallicities, we have demonstrated that the near-IR features cannot be reproduced with models at appropriate metallicities.

Different assumptions for the IMF do not change the conclusion, as one can see in Fig. 4 where we compare models with both a Salpeter and a Miller-Scalo IMF (approximated as a power-law with index 3.30). The results are very similar at both $Z = 0.020$ and $Z = 0.008$. The negligible dependence on the IMF simply follows from the fact that RSGs provide both the line flux and the adjacent continuum. Therefore the IR indices sample a relative small stellar mass interval. This is very different from, e.g., stellar-wind lines in the UV or the Wolf-Rayet feature at $\lambda 4686 \text{ \AA}$ (cf. Leitherer et al. 1995; Schaerer & Vacca 1998).

Different assumptions for the model of at-

mospheres do not change the result, either. When we built the OMO93 code we performed tests to investigate how the choice of the adopted model of atmosphere for given stellar parameters influences the computed equivalent widths. No significant dependence on the adopted model atmospheres was found. The main reason is simply the fact that the main source of opacity in late type stars is the H^- ion. We also performed test calculations with our L98 code, which has the capability to model cool stars with Kurucz or Lejeune models, or with blackbodies. All three choices uniformly give the same result: too weak RSG features. As we will demonstrate below, the dominant effect is the failure of the evolutionary models which predict incorrect RSG parameters. The failure is so severe that the details of the model atmospheres become negligible.

To understand why the model spectra differ from those of real stellar clusters and galaxies, we should explore how RSGs affect the integrated light. Before the first RSGs form, the near-IR spectrum will be dominated by emission from ionized gas. The UV spectrum is dominated by the photospheric emission from O-B stars. Once these stars begin to turn off the main sequence, they become massive RSGs and dominate the near-IR spectrum in the range of ages between 8–30 Myr (involving stars of mass ~ 25 – $10 M_{\odot}$). Actually the evolution of intermediate mass RSGs (~ 5 – $15 M_{\odot}$) is more complex since these stars also have blue excursions towards higher temperatures which may last a large fraction ($\geq 50\%$) of the total core-helium burning phase, particularly at low metallicities.

During the RSG phase the integrated colors of the evolving stellar population should

become red and the absorption features typical of cool stars deep, but how much red and deep depends on their average temperature and blue-loop duration, which in turn depends on many factors (metallicity, mass loss rate etc.)

In order to better identify the possible cause of the mismatch between predicted and observed IR features, we computed near-IR indices and colors of *individual stars* predicted by the evolutionary models instead of considering an entire population. The mass range of the relevant contributors to the IR indices and colors at ages ≤ 30 Myr is roughly 25 to $8 M_{\odot}$. Fig. 5 shows the predicted CO indices of a 25, 20, 15, 12, 10 and $8 M_{\odot}$ star for solar and 40% solar metallicity.

The Z_{\odot} models (cf. Fig. 5, left panels) for 25, 20 and $15 M_{\odot}$ reach the RSG stage at $\simeq 6.5$, 8.5 and 12 Myr, respectively, when the equivalent widths start to peak. About 1 Myr later the RSGs explode as supernovae, and the CO feature is no longer observed. The duration of the RSG phase increases with decreasing main-sequence mass as indicated by the broader equivalent width peak at $15 M_{\odot}$ as compared to that at 25 and $20 M_{\odot}$. A qualitative change of this behavior occurs for stars with masses smaller than $12 M_{\odot}$. The 8–12 M_{\odot} models at Z_{\odot} have two peaks, separated by a more than 1 Myr long gap of zero equivalent width. The gap is caused by a blue loop in the evolutionary models, when temperatures above 10,000 K are reached, too high to produce any CO feature. Since RSGs have a blue excursion lasting about 50% of the entire RSG lifetime, no CO features are predicted during about 50% of the RSG lifetime for masses below about $15 M_{\odot}$.

Next we consider stars with $0.4 Z_{\odot}$ (cf. Fig. 5, right panels). The resulting models

produce lower equivalent widths than at solar metallicity. Three main reasons can explain such a behavior: at lower Z the effective temperature of RSGs is higher, blue loops start at larger masses ($\sim 15 M_{\odot}$), and they last longer (about 20% more). The offset in time between the indices of stars having the same mass but different Z is due to slower evolution at lower Z (Maeder 1990).

In an instantaneous burst, integration over all mass ranges will lead to the prediction that the presence or absence of blue loops significantly affects the line equivalent widths and the $(J - K)$ color of a RSG population, while it does not severely contaminate the optical colors. A clear example of this prediction is the discontinuity at about 14 Myr in the instantaneous burst models of the infrared features, where the equivalent widths of the absorption lines drop and the $(J - K)$ color turns blue for a short period of time (see Figs. 1 and 2). This discontinuity is also present in the solar models but it is less obvious since blue loops are more pronounced at low metallicity.

Cases for continuous star formation are affected to a much smaller degree: the main contributor to the line equivalent width has a main-sequence mass of $15 M_{\odot}$ and above, and such stars do not have blue loops.

As a result of the warm temperatures and very pronounced blue loops at sub-solar Z in the Geneva models, the equivalent widths of the absorption features and the $(J - K)$ color cannot approach the values observed in the clusters. Mayya (1997) already reached similar conclusions for the $(J - K)$ color. OO98, using different models based on Padova evolutionary tracks (Bertelli et al. 1994), also found that at low Z the models predict too warm temperatures for the RSGs.

Stars on blue loops, which are still cooler

than the more massive blue supergiants in an earlier evolutionary stage, significantly contribute to the $(U - B)$ color (mainly to the B luminosity) in an instantaneous burst. This makes the $(U - B)$ redder. The continuous star formation models predict much bluer $(U - B)$ than the instantaneous ones since the blue-loop stars are less dominant. Moreover, the presence of the blue loops may also account for the apparent reddening of the $(U - B)$ color when metallicity decreases since the blue loops become progressively more pronounced.

While Meynet (1993) and Mayya (1997) suggested that perhaps changing the mass-loss rate could provide a solution, we have taken a more general approach. In an attempt to provide guidance to the stellar evolution groups, we now derive empirical limits on the RSG temperatures and the fraction of the core-helium burning lifetimes the massive stars spent as RSGs (vs. time spent in blue loops, or as blue supergiants).

4. Results from the modified models

4.1. Theoretical background

There are a number of plausible reasons why the theoretical predictions in the near-IR do not match the observed RSG populations.

The coolest temperatures predicted by evolutionary models for RSGs of fairly high mass ($M > 10 M_{\odot}$) are quite uncertain. The major uncertainty stems from the treatment of the external convective layers in these stars. As discussed by Maeder (1987), the treatment of non-adiabatic convection with the usual mixing length theory (MLT) leads to supersonic convective velocities, which is in contradiction to assumptions of this theory. To remedy this situation one includes (cf. Schaller

et al. 1992) the contribution of the acoustic flux to the energy transport and the turbulent pressure in the hydrostatic equilibrium. Furthermore, a density scale height is adopted to prevent density inversions. The difference between this treatment and the usual MLT is illustrated by Maeder & Meynet (1987, their Fig. 9) and by Chiosi et al. (1992). In view of these uncertainties, the predictions for both the effective temperatures of RSGs and their dependence on metallicity have to be regarded as considerably uncertain. This most likely explains the difficulties of evolutionary models to correctly reproduce the radii and temperatures of massive RSGs. Future progress will be required to reliably model the extreme conditions in these convective envelopes.

Another crucial difference is the amount of time spent as a RSG during the core–helium burning phase. At solar metallicity a supergiant star spends a large fraction of its core–helium burning phase in the red near the coolest position it will reach on the HRD. As metallicity decreases, more and more of the core–helium burning lifetime is spent at significantly higher temperatures ($\geq 10^4$ K), where these objects will presumably be classified as blue supergiants. It is well known that the transition between blue and red supergiants is particularly sensitive to different model ingredients (internal mixing, mass loss, opacities etc.; e.g., Maeder & Meynet 1988; Ritossa 1996). As discussed in detail by Langer & Maeder (1995) no current set of evolutionary models is able to reproduce correctly the *variation* of the observed ratio of blue to red supergiants with metallicity.

4.2. Models with empirically adjusted RSG parameters

Given the above situation, we explored a set of models where the stellar effective temperature and the fraction of time spent by a massive star in the red part of the HRD during the core–helium burning phase are free parameters. This should allow us to better quantify the role played by these parameters in the overall spectral properties of the selected indices and to provide feedback constraints on the evolutionary tracks of massive stars. We ran models at $Z = 0.008$ fixing the fraction of time during the core–helium burning phase spent in the red (i.e. as RSG) at 10%, 50% and 98% and the RSG temperature at 3500 K, 4000 K, and 4500 K, regardless its mass. The temperature and lifetime adjustments were performed as follows: for all time steps on the evolutionary track after the step corresponding to 90%, 50%, or 2% of the total core–helium lifetime, the temperature was settled to 3500K, 4000K, or 4500K.

The main results are shown in Figs. 6–11 for the CO features with both solar and sub-solar [C/Fe], ($U - B$) and ($J - K$) color models, for both an instantaneous burst and continuous star formation. The behavior of the CO feature at $\lambda 1.62$ indicates that the observed values of young LMC clusters can be reproduced by 40% solar metallicity models only in a limited range of parameters. Temperatures < 4000 K and fraction of time spent in the red during the core–helium burning phase of at least $\sim 50\%$ are required. These can be regarded as upper and lower limits, respectively, when models with carbon depletion are considered. For the galaxies, similar temperatures and lifetimes are required. It is also interesting to note that the discontinuity around 14 Myr progressively disappears when

increasing the time spent in the red, also in better agreement with the modeling based on the Padova evolutionary tracks (cf. Oo98). This is a clear indication that the discontinuity can be simply an artifact due to the blue loops and has nothing to do with the actual temporal evolution of the integrated stellar population.

The CO at $\lambda 2.29$ is a less sensitive thermometer than the CO at $\lambda 1.62$ but its behavior is fully consistent with the trends shown by the latter (cf. Figs. 8 and 9). The analysis of the colors supports the temperature/RSG lifetime conclusions from the spectroscopic features. Only in the same temperature/RSG lifetime regime which can account for the indices, do we approach the $(J - K) = 0.8 - 1$ needed to account for the observations of clusters and galaxies (cf. Fig. 11).

The $(U - B)$ color (cf. Fig. 10) becomes slightly bluer both increasing the lifetime and decreasing the temperature of RSGs. This behavior is the confirmation that blue loops being cooler than the bluest supergiants but significantly warmer than the RSGs have the net effect to make the $(U - B)$ redder and the $(J - K)$ colors bluer. Going to lower temperatures and longer lifetimes in the RSG phase cause the models to have only very blue and very red stellar populations dominating the luminosity in the UV to blue and in the infrared domain, respectively, in better agreement with the observed features.

Fractions of time spent in the red during the core-helium burning phase larger than 50% imply a ratio of blue to red supergiants less than 1. Direct estimates of this ratio from observed color-magnitude diagrams (CMDs) are very rare and severely affected by statistical effects. Nevertheless in the few published CMDs of young LMC clusters there is evi-

dence that this ratio is truly ≤ 1 even at relative low metallicities (e.g., Chiosi et al. 1995 for NGC330 and Balona & Jerzykiewicz 1993 for NGC2004 and NGC2100). More efforts should be made to obtain a larger sample of reliable CMDs of young LMC clusters to provide the ratio of blue to red supergiants with much higher statistical significance.

As shown by Mayya (1997) the observed Ca II triplet, $(J - K)$ color and photometric CO index of a sample of young LMC clusters are better reproduced by models which enhance the mass loss by a factor of two with respect to the standard RSG model. However, the photometric CO index is still less than observed, and the UV-optical colors become redder than the observed ones. This indicates that mass loss cannot be the single cause for the discrepancy and other crucial parameters most likely play a major role, as discussed in Sect. 4.1. Unless more details in the evolution of RSGs become clearer, any diagnostics which involve temporal evolution of the IR features is still too premature. For example the predicted decreases of the Ca II triplet equivalent width and the CO photometric index in the age range between 12 and 100 Myr is most probably an artifact of too-pronounced blue loops in the Geneva evolutionary tracks.

5. Conclusions

The key results of this study are:

- Evolutionary tracks of RSGs can reasonably account for the observed optical features but fail to reproduce the observed $(U - B)$ color and the IR spectra of stellar clusters and starburst galaxies at *sub-solar metallicity*. They do not produce sufficiently cool super-

giants with long enough core–helium burning phase in the red part of the HRD.

- The high sensitivity of the selected spectroscopic indices to the physical parameters of cool stars make the present simulations a powerful tool to place constraints on the temperature and fraction of time spent in the red: at 40% solar metallicity, the former should be less than 4000 K, and the latter at least 50%.
- Synthesis models for the burst evolution which use IR diagnostics of massive red stars with sub–solar metallicity are still unreliable due to deficiencies in stellar evolution models.
- Models with empirically adjusted RSG parameters allow a reasonable fit for both the observed UV to blue and IR features in young stellar clusters and starburst galaxies.
- The full model set, with original RSG parameters at Z_{\odot} and with empirical adjustments at 40% Z_{\odot} is available in electronic form at <http://www.stsci.edu/ftp/science/starburst>.

Livia Origlia gratefully acknowledges financial support from the STScI Visitor Program. Funding for Jeff Goldader was provided by NASA grant GO–06672.01–95A from the Space Telescope Science Institute, operated by the Association of Universities for Research in Astronomy, Inc., under NASA contract NAS5-2655. Claus Leitherer received financial support from the Visiting Professor Program of the University of Bologna. Salary

support for Daniel Schaerer was provided by the STScI Director’s Discretionary Research Fund. The authors acknowledge the anonymous referee for the helpful comments and suggestions.

REFERENCES

- Abbott, D. C., & Conti, P. S. 1987, *ARA&A*, 25, 113
- Arimoto, N., Matsushita K., Ishimaru, Y., Ohashi, T., & Renzini, A. 1997, *ApJ*, 477, 128
- Balona, L. A., & Jerzykiewicz, M. 1993, *MNRAS*, 260, 782
- Bica, E., Alloin, D., & Santos, J. F. C. Jr. 1990, *A&A*, 235, 103
- Bertelli, G., Bressan, A., Chiosi, C., Fagotto, F., & Nasi, E. 1994, *A&AS*, 106, 275
- Bruzual A., G., & Charlot, S. 1993, *ApJ*, 405, 538
- Carral, P., Hollenbach, D. J., Lord, S. D., Colgan, S. W. J., Haas, M. R., Rubin, R. H., & Erickson, E. F. 1994, *ApJ*, 423, 223
- Cassatella, A., Barbero, J., Brocato, E., Castellani, V., & Geyer, E. H. 1996, *A&A*, 306, 125
- Chiosi, C., Bertelli, G., & Bressan, A. 1992, *ARA&A*, 30, 235
- Chiosi, C., Vallenari, A., Bressan, A., Deng, L., & Ortolani, S. 1995, *A&A*, 293, 710
- Conti, P. 1991, *ApJ*, 377, 115
- Elson, R. A. W., & Fall, S. M. 1985, *ApJ*, 299, 211
- . 1988, *AJ*, 96, 1383
- García–Vargas, M. L., González–Delgado, R. M., Pérez, E., Alloin, D., Díaz, A., & Terlevich, E. 1994, *ApJ*, 478, 112

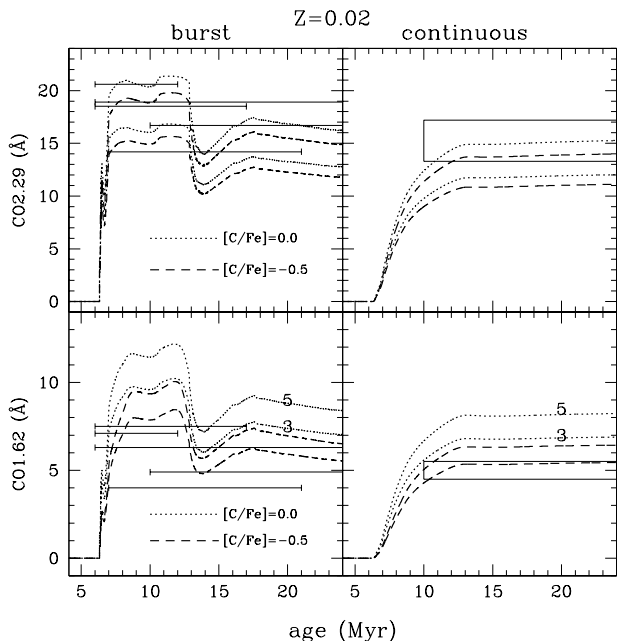


Fig. 1.— The behavior of the CO spectroscopic features for instantaneous burst (left panels) and continuous star formation models (right panels) using a Salpeter IMF, solar metallicity, microturbulent velocity ξ of 3 and 5 km/s, solar $[C/Fe]$ (dotted lines), one third solar $[C/Fe]$ (dashed lines). The CO $\lambda 2.29$ is related to photometric CO index by the empirical relations (Kleinmann & Hall 1986 and Origlia et al. 1997):

$$[CO]_{\text{spec}} = -2.5 \log \left[1 - \frac{W_{\lambda}(2.29)}{53\text{\AA}} \right];$$

$$[CO]_{\text{phot}} \simeq -0.6 \times [CO]_{\text{spec}} - 0.017.$$

For the instantaneous burst models we also show the values measured in a sample of young LMC clusters (cf. OO98), while in the continuous star formation models the rectangular boxes indicate the range of values ($\pm 1\sigma$) measured in a sample of starburst galaxies by Oliva et al. (1995).

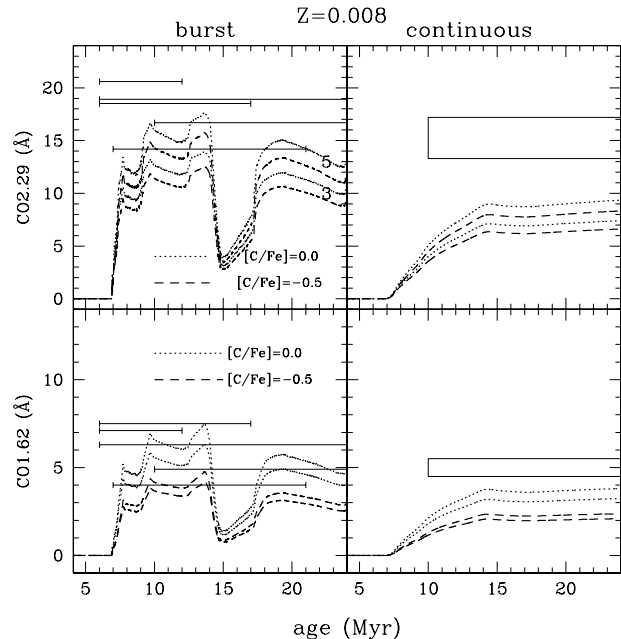


Fig. 2.— As in Fig. 1, but for 40% solar metallicity.

- Girardi, L., Chiosi, C., Bertelli, G., & Bresnan, A. 1995, *A&A*, 298, 87
- Glass, I. S., & Moorwood, A. F. M. 1985, *MNRAS*, 214, 429
- Goldader, J. D., Joseph, R. D., Doyon, R., & Sanders, D. B. 1995, *ApJ*, 444, 97
- . 1997, *ApJS*, 108, 449
- González-Delgado, R. M., Pérez, E., García-Vargas, M. L., Terlevich, E., & Vílchez, J. M. 1994, *ApJ*, 439, 604
- Hamuy, M., & Maza, J. 1987, *A&AS*, 68, 383
- Jasniewicz, G., & Thévenin, F. 1994, *A&A*, 282, 717
- Kleinmann, S. G., & Hall, D. N. B., 1986, *ApJS*, 62, 501
- Lamb, S. A., Gallagher, J. S., Hjellming, M. S., & Hunter, D. A. 1985, *ApJ*, 291, 63

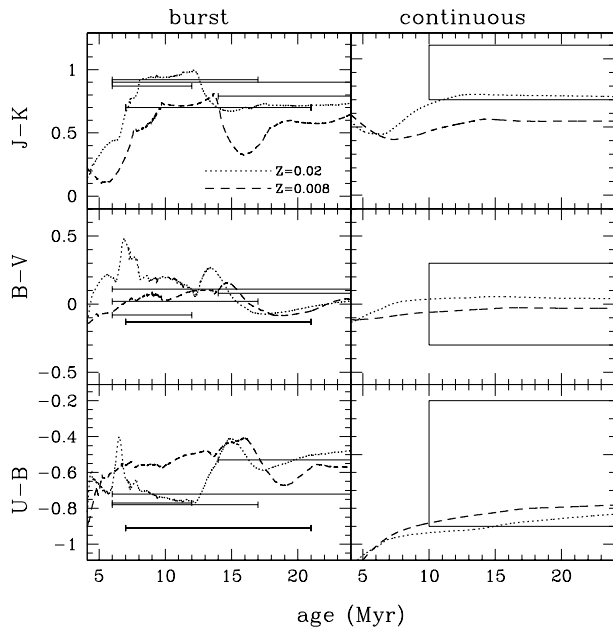


Fig. 3.— Colors of the standard burst (left panels) and continuous star formation (right panels) models with $Z = 0.020$ (dotted lines) and $Z = 0.008$ (dashed lines). As in Figures 1 and 2, the de-reddened values of a sample of LMC clusters and starburst galaxies (boxes) are also shown for comparison. The boxes indicate the range of values computed for the galaxies, assuming uncertainties in the adopted A_V of ± 0.5 mag.

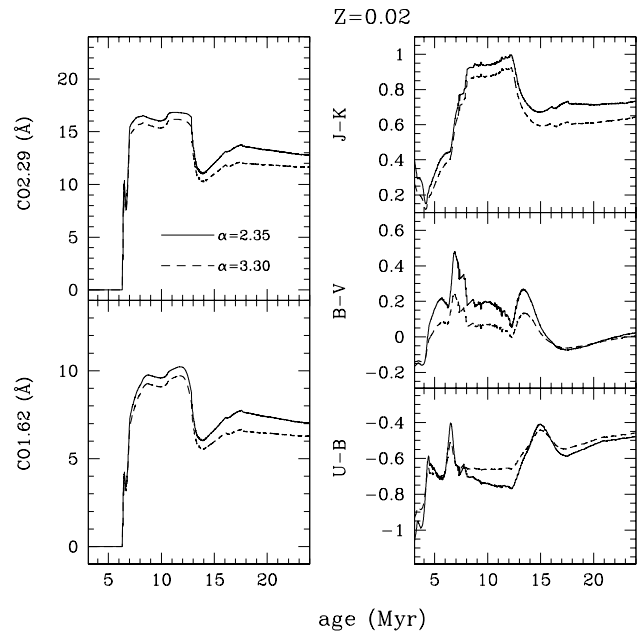


Fig. 4.— Comparison between burst models with standard Salpeter (continuous lines) and Miller-Scalo (dashed lines, approximated by a power-law slope of 3.30) IMFs at $Z = 0.02$. Differences in the IMF have very little effect on the strengths of both the spectroscopic indices and colors.

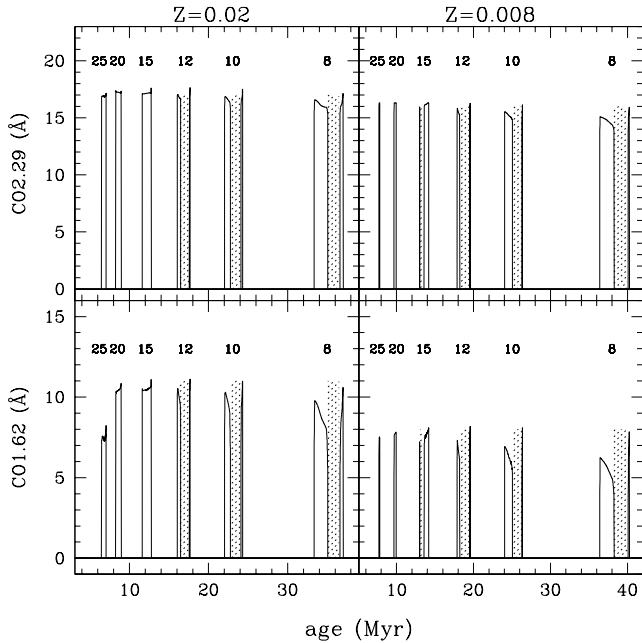


Fig. 5.— Instantaneous burst models for the CO features, taking into account only the contribution of RSGs with single masses: 25, 20, 15, 10 and 8 M_{\odot} , respectively, at $Z = 0.02$ (left panels) and $Z = 0.008$ (right panels). The shaded regions correspond to the blue loops.

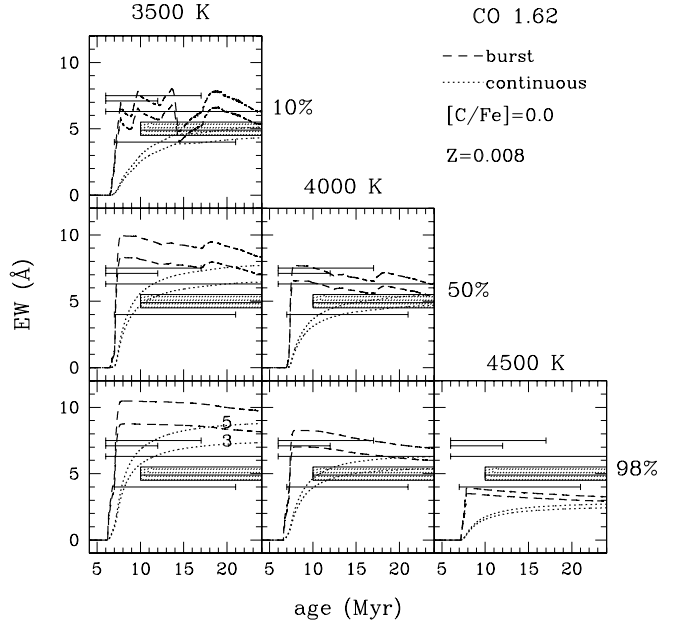


Fig. 6.— Modified models for the CO $\lambda 1.62$ index, where we have empirically adjusted the RSG temperature and lifetime during the core–helium burning phase. The temperature is displayed at the top of the panels while the fraction of time spent as a RSG is displayed on the right side. In each panel, we show the instantaneous burst (dotted lines) and continuous star formation (dashed lines) models at $Z = 0.008$, solar $[C/Fe]$ relative abundance and assume a Salpeter IMF. The de–reddened values of young LMC clusters and starburst galaxies (shaded rectangles) are also plotted for comparison.

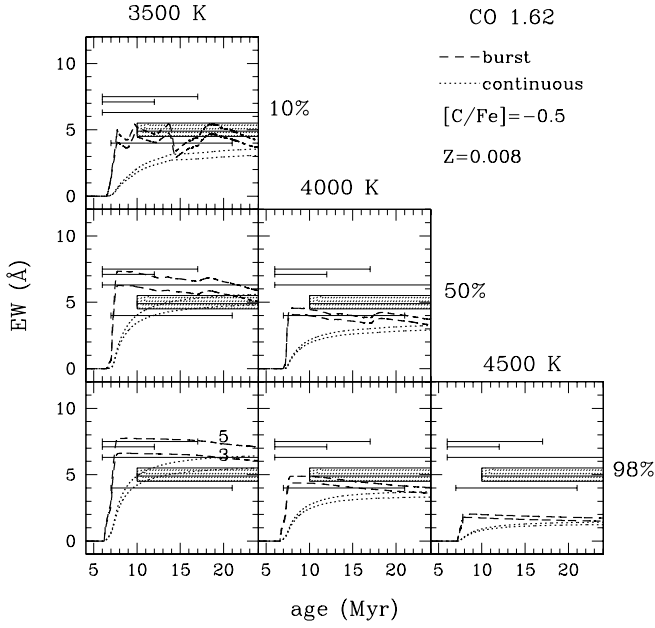


Fig. 7.— As in Fig. 6, but for a $[C/Fe] = -0.5$.

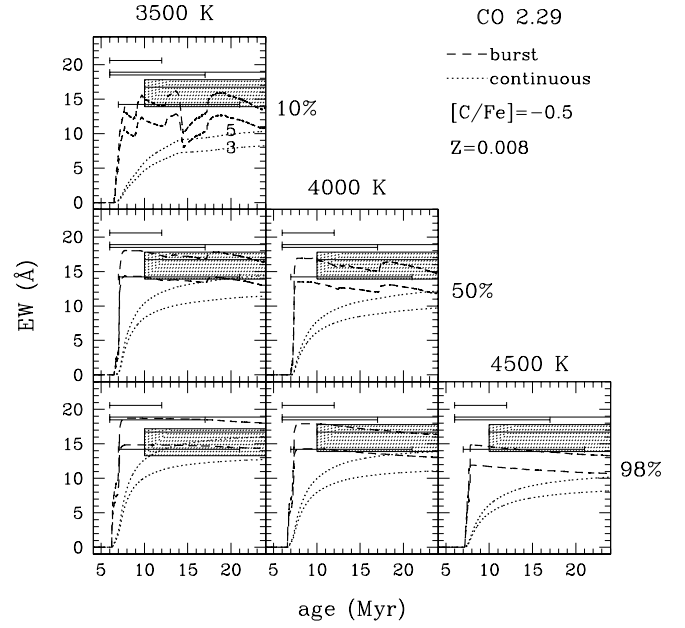


Fig. 9.— As in Fig. 8, but for a $[C/Fe] = -0.5$.

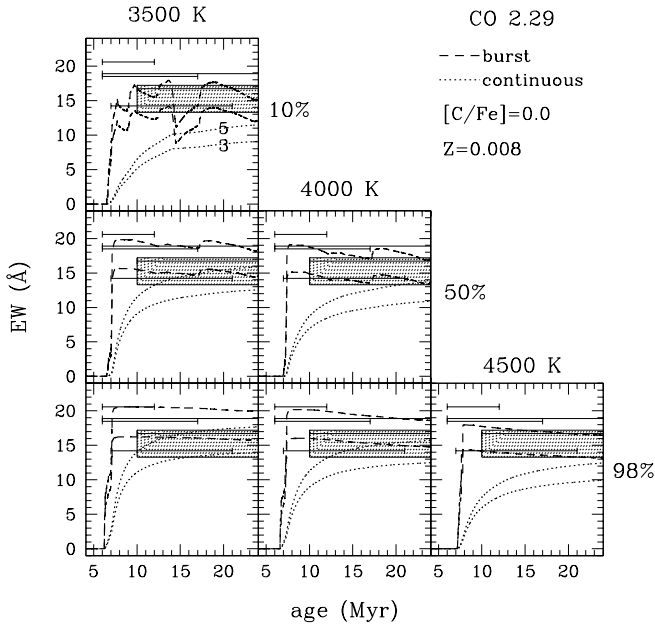


Fig. 8.— As in Fig. 6, but for the CO $\lambda 2.29$ index.

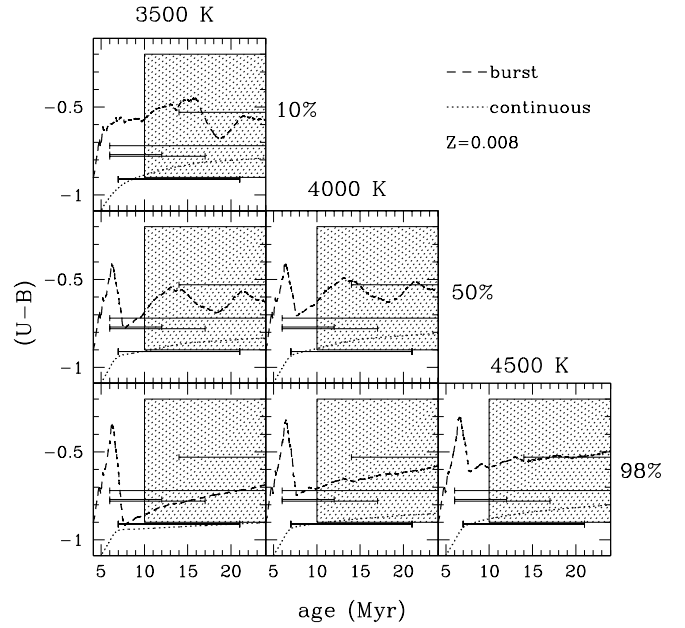


Fig. 10.— As in Fig. 6 but for the $(U - B)$ colors.

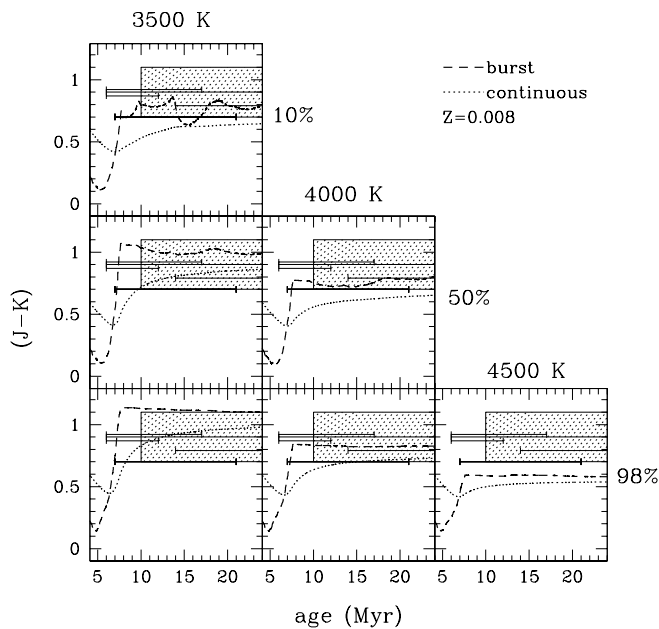


Fig. 11.— As in Fig. 6, but for the $(J - K)$ colors.

Lambert, D. L., Brown, J. A., Hinkle, K. H., & Johnson, H. R. 1984, *ApJ*, 284, 223

Lançon, A., & Rocca-Volmerange, B. 1992, *A&AS*, 96, 593

Langer, N., & Maeder, A. 1995, *A&A*, 295, 685

Leitherer, C. 1996, in *From Stars to Galaxies*, ASP Conf. Ser. 108, eds. C. Leitherer, U. Fritze-von Alvensleben, & J. Huchra (San Francisco:ASP), 373

Leitherer, C., & Heckman, T. M. 1995, *ApJS*, 96, 9 (LH95)

Leitherer, C., Robert, C., & Heckman, T. M. 1995, *ApJS*, 99, 173

Leitherer, C., Schaerer, D., Goldader, J. D., González-Delgado, R. M., Robert, C., Foo Kune, D., de Mello, D. F., Devost, D., & Heckman, T. M. 1998, *ApJS*, submitted (L98)

Leitherer, C., et al. 1996, *PASP*, 108, 996

Lejeune, T., Cuisinier, F., & Buser, R. 1997, *A&AS*, 125, 229

Maeder, A., 1987, *A&A*, 173, 247

———. 1990, *A&AS*, 84, 139

Maeder, A., & Meynet, G. 1987, *A&A*, 182, 243

Mayya, Y. D. 1997, *ApJ*, 482, 149

Meynet, G. 1995, *A&A*, 298, 767

———. 1995, in *The Feedback of Chemical Evolution on the Stellar Content of Galaxies*, 3rd DAEC Meeting, eds. D. Alloin, & G. Stasińska, Publ. Obs. Paris, 40

Miller, G. E., & Scalo, J. M. 1979, *ApJS*, 41, 513

Moorwood, A. F. M. 1996, *Space Science Reviews*, 77, 303

Oliva, E., & Origlia, L. 1998, *A&A*, 332, 46 (OO98)

Oliva, E., Origlia, L., Kotilainen, J. K., & Moorwood, A. F. M. 1995, *A&A*, 301, 55

Origlia, L., Ferraro, F. R., Fusi Pecci, F., & Oliva, E. 1997, *A&A*, 321, 859

Origlia, L., Moorwood, A. F. M., & Oliva, E. 1993, *A&A*, 280, 536 (OMO93)

Persson, S., Aaronson, M., Cohen, J., Frogel, J., & Matthews, K. 1983, *ApJ*, 266, 105

Ptak, A., Serlemitsos, P., Yaqoob, T., Mushotzky, R., & Tsuru, T. 1997, *AJ*, 113, 1286

Quillen, A. C., Ramirez, S. S. V., & Frogel, J. A. 1995, *AJ*, 110, 205

Reitermann, A., Baschek, B., Stahl, O., & Wolf, B. 1989, *A&A*, 234, 109

Renzini, A. 1986, in *Stellar Populations*, Conf. Ser. 108, eds. C. A. Norman, A. Renzini, & M. Tosi (Cambridge: CUP), 213

- Richtler, T., Spite, M., & Spite, F. 1989, A&A, 225, 351
- Rieke, G. H., & Lebofsky, M. J. 1985, ApJ, 288, 618
- Ritossa, C. 1996, MNRAS, 281, 970
- Salpeter, E. E. 1955, ApJ, 121, 161
- Schaerer, D., & Vacca, W. D. 1998, ApJ, 497, 618
- Schaller, G., Schaerer, D., Meynet, G., & Maeder, A. 1992, A&AS, 96, 269
- Scoville, N. Z., Soifer, B. T., Neugebauer, G., Young, J. S., Matthews, K., & Yerka, J. 1985, ApJ, 289, 129
- Searle, L., Sargent, W. L. W., & Bagnuolo, W. G. 1973, ApJ, 179, 427
- Smith, D. A., Terry, H., Haynes, M. P., Beichman, C. A., & Gautier, T. N. 1996, ApJS, 104, 217
- Storchi-Bergmann, T., Calzetti, D., & Kinney, A. L. 1994, ApJ, 429, 572
- Tinsley, B. M. 1972, A&A, 20, 383
- Tsuji T., Ohnaka, K., Hinkle, K. H., Ridgway S. T. 1994, A&A, 289, 469
- van den Bergh, S. 1981, ApJS, 46, 79
- Veron-Cetty, M. P. 1984, A&AS, 58, 665
- Webster, B. L., & Smith, M. G. 1983, MNRAS, 204, 743
- Worthey, G. 1994, ApJS, 95, 107
- Zaritsky, D., Kennicutt, Jr., R. C., & Huchra, J. P. 1994, ApJ, 420, 87